A Heat Transfer Model for the Production of Semi-Solid Billets With the SEED Process
Colbert, Josée; Bouchard, Dominique

National Research Council Canada   Conseil national de recherches Canada

Canada

A Heat Transfer Model for the Production of Semi-Solid Billets with the SEED Process

Josée Colbert[1,2,a] and Dominique Bouchard[1,b]

[1]Aluminum Technology Center, National Research Council of Canada, 501 boul. de l'Université Est, Chicoutimi, QC, Canada, G7H 8C3
[2]Université du Québec à Chicoutimi, 555 boul. de l'Université Est, Chicoutimi, QC, Canada, G7H 2B1
[a] josee.colbert@imi.cnrc-nrc.gc.ca, [b] dominique.bouchard@imi.cnrc-nrc.gc.ca

Keywords: Semi-solid aluminum, SEED, heat transfer coefficient, inverse heat conduction, empirical model, numerical simulations

Abstract

A heat transfer model was built to predict the temperature evolution of semi-solid aluminum billets produced with the SEED process. An inverse technique was used to characterize the heat transfer coefficient at the interface between the crucible and the semi-solid billet. The effect of several process parameters on the heat transfer coefficient was investigated with a design of experiments and the coefficient was inserted in a computer model. Numerical simulations were carried out and validated with experimental results.

Introduction

A great deal of research and development has been devoted over the years to die cast semi-solid aluminum [1]. This is explained by the high integrity components that are obtained, compared to the conventional casting of liquid metal. Thixocasting and rheocasting are two different routes to produce castings from semi-solid aluminum and both process a feedstock having a globular structure. With thixocasting, liquid aluminum is first solidified into bar stock in the presence of mechanical or magnetic agitation. The bars are then sliced into billets and heated in the semi-solid condition before their injection in a die-casting press. Rheocasting is simpler since it only has two basic steps. Liquid metal is brought into the solid-liquid temperature range and injected in the press [1].

The process using the Swirled Enthalpy Equilibration Device (SEED) belongs to the rheocasting family. Details in the preparation of semi-solid billets with this process patented by Alcan International Limited have been given elsewhere [2, 3, 4] but basically consist of cooling a poured amount of liquid metal in a swirling crucible followed by draining. During cooling, the heat loss in the aluminum is mainly controlled by the crucible material and mass. Their proper selection is thus instrumental to ensure that the slurry has the desired combination of temperature and solid fraction. When selecting a crucible, heat transfer simulations are valuable to reduce the number of costly and time consuming experimental trials. A heat transfer analysis of SEED has already been reported for a single billet dimension and fixed process parameters [5]. The objective of this study is to develop a more general computer model that simulates heat flow prior to drainage and to predict requirements for crucibles at various billet dimensions and process conditions for the A356 alloy.

Theory

Heat Transfer: In the SEED process, the heat supplied by the aluminum is mainly absorbed by the crucible and some by the ambient air. Conduction is the main transport mode but convection and radiation are also present. Figure 1 depicts the crucible and the aluminum along with boundary conditions involving the aluminum, the crucible and the ambient air. The bottom of the crucible

consists of refractory material and the refractory/billet interface may be treated as an adiabatic boundary.
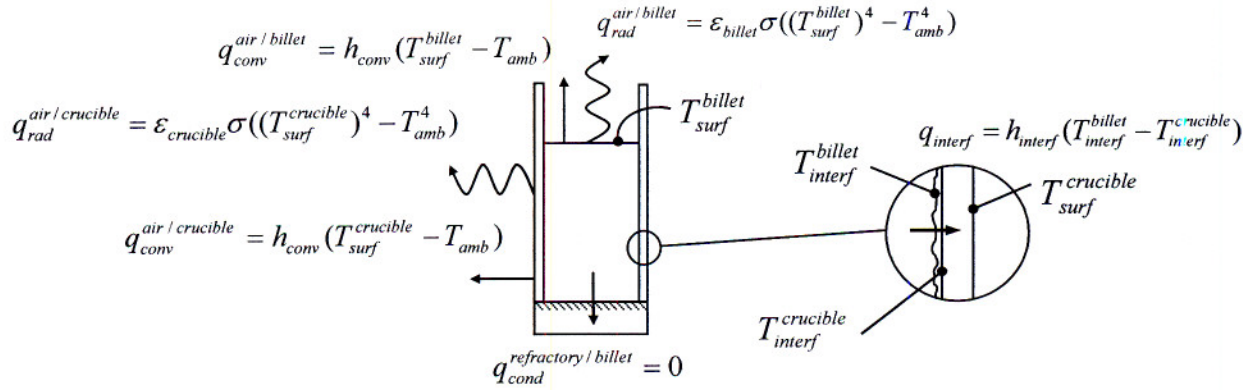

Figure 1 : Schematic view of the billet and the crucible. Boundary conditions to perform numerical simulations of the heat flow are also shown. Their parameters are all known except the heat transfer coefficient at the interface between the billet and the crucible, h_{interf}, illustrated in the zoomed portion. This coefficient was evaluated in this study.

The temperature evolution in the crucible and the billet may be calculated by solving the unsteady state heat conduction equation. Due to symmetry, a two dimensional expression in cylindrical coordinates of the longitudinal half is sufficient. For the crucible, the unsteady state heat conduction equation is:

$$\frac{1}{r}\frac{\partial}{\partial r}\left(r \cdot k \frac{\partial T}{\partial r}\right) + \frac{\partial}{\partial z}\left(k \frac{\partial T}{\partial z}\right) = \rho C_p \frac{\partial T}{\partial t} . \tag{1}$$

For the aluminum, an enthalpy formulation [6] of Equation (1) is utilized to deal with the phase transformation. The swirling of the crucible also produces motion of the aluminum that enhances the heat flow and this effect can be accounted in the model by using an effective thermal conductivity [7], k_{eff}, for the liquid phase such that $k_{eff} = k_c \cdot k(T)$. The value of the multiplying factor k_c in this equation is typically between 5 and 10 and $k(T)$ is the thermal conductivity of the solid. A commercial finite element software, ProCAST[TM], was used to solve equation (1) for the crucible and the billet. The materials properties required by this equation were taken from the ProCAST[TM] databank. Initial and boundary conditions must however be applied in the utilization of such finite element software. The initial temperatures of the crucible and the aluminum are process parameters selected by the user. The radiation boundary conditions require values for the emissivity of the crucible and the aluminum. Those used for the study were respectively: 0.75, 0.8 and 0.15 for the two different crucibles and the aluminum alloy [8] that were tested. The convection boundary conditions require heat transfer coefficients at the air/crucible and air/billet interfaces and for processes undergoing free convection such coefficients typically vary between 5 and 25 W/m^{2}K [9]. A value of 25 W/m^{2}K was used here to account for the eccentric movement of the crucible caused by swirling.

The crucible/billet interface is also treated as a boundary condition that requires a heat transfer coefficient. This coefficient was characterized by solving an inverse heat conduction problem (IHCP) using a methodology developed by Beck [10]. The methodology can be summarized in four steps: 1) temperatures are measured apart from the interface, 2) the interfacial heat flux per unit area, q, that reproduces the measurements is solved, 3) the surface temperatures of the two portions

that compose the interface are calculated using that flux as a boundary condition, 4) the interfacial heat transfer coefficient, h_{interf}, is obtained by applying Newton's law of cooling. In step 2), the heat flux per unit area, q, is solved at each time step with the following iterative formula:

$$q_m^{n+1} = q_m^n + \frac{\sum_{i=1}^{r}\sum_{j=1}^{J}\left[Y_{m+i-1,j} - T_{m+i-1,j}(q_m^n)\right]\cdot\left[\left(T_{m+i-1,j}(q_m^n(1+\delta)) - T_{m+i-1,j}(q_m^n)\right)/\delta q_m^n\right]}{\sum_{i=1}^{r}\sum_{j=1}^{J}\left[\left(T_{m+i-1,j}(q_m^n(1+\delta)) - T_{m+i-1,j}(q_m^n)\right)/\delta q_m^n\right]^2}. \quad (2)$$

In this expression, J is the number of thermocouples and r is the number of future time step. δ is a small quantity that increments q_m^n and its superscript 'n' refers to the nth iteration and 'm' is a time index. $Y_{m+i-1,j}$ corresponds to the measured temperature at the time interval $m+i-1$ with sensor j. Calculated temperatures for that sensor, for an imposed interfacial heat flux q_m^n and $q_m^n(1+\delta)$, are represented by $T_{m+i-1,j}(q_m^n)$ and $T_{m+i-1,j}(q_m^n(1+\delta))$, respectively. Equation 2 is iterated until the relative difference between q_m^{n+1} and q_m^n is small. At this point, the solution for the heat flux at time index 'm', has converged. Steps 3) and 4) are then performed and the sequence of calculations is repeated for the next time index.

Design of Experiments (DoE): Several experimental factors affect the evolution of the heat transfer coefficient at the interface between the crucible and the billet. Some of them may be more significant than others and their independent evaluation would require a large number of experiments. Design of experiments, (DoE) [11], was used in this work to identify the significant factors and to reduce the number of trials required to evaluate the response variables, in occurrence, the interfacial heat transfer coefficient. In this study, 9 experimental factors of the SEED process were investigated at 2 different levels with a Taguchi design consisting of 16 experiments and 15 degrees of freedom (L16). The list of experimental factors and their levels is given in Table 1 .

Experiment number	A:Crucible initial temperature [°C]	B:Aluminum pouring temperature [°C]	C:Bottom plate initial temperature [°C]	D:Crucible materials*	E:Draining grids*	F:Coating materials*	G:Bottom plates*	H:Crucible wall thickness [mm]	I:Coating thickness [μm]
1	25	645	25	CM1	G1	C1	P1	1.85	30
2	25	645	25	CM2	G2	C2	P1	3.25	30
3	25	645	100	CM1	G2	C2	P2	1.85	60
4	25	645	100	CM2	G1	C1	P2	3.25	60
5	25	685	25	CM1	G2	C2	P2	3.25	60
6	25	685	25	CM2	G1	C1	P2	1.85	60
7	25	685	100	CM1	G1	C1	P1	3.25	30
8	25	685	100	CM2	G2	C2	P1	1.85	30
9	75	645	25	CM1	G2	C1	P1	3.25	60
10	75	645	25	CM2	G1	C2	P1	1.85	60
11	75	645	100	CM1	G1	C2	P2	3.25	30
12	75	645	100	CM2	G2	C1	P2	1.85	30
13	75	685	25	CM1	G1	C2	P2	1.85	30
14	75	685	25	CM2	G2	C1	P2	3.25	30
15	75	685	100	CM1	G2	C1	P1	1.85	60
16	75	685	100	CM2	G1	C2	P1	3.25	60

* Proprietary SEED components. Coatings are applied inside the crucibles.

Table 1 : List of experimental factors (*A* to *I*) with corresponding levels in the experimental design.

As mentioned earlier, the heat transfer coefficient was treated as the response variable subject to the experimental factors. Figure 2 illustrates a typical qualitative evolution of this coefficient for a metal solidifying on a mold wall [12,13]. It is characterized by a transient regime having a relatively rapid rise and fall with an exponential decay followed by a steady state regime having a more stable value. This behavior is approximated by the set of three solid lines on the graph; one for the rise, another for the fall and the last for the stable value. The dotted line can be fairly reconstructed from the knowledge of the following principal parameters: the initial value, h_o, occurring at $t_o = 0$, the peak value h_1, occurring at t_1 and the steady state value, h_2, occurring at t_2. Therefore, the experimental design treated 5 response variables: h_o, h_1, h_2, t_1, and t_2. Linear regressions were also performed on the collected data to yield empirical models for these response variables. From these models, an entire heat transfer coefficient curve could be reproduced for a given set of experimental condition.
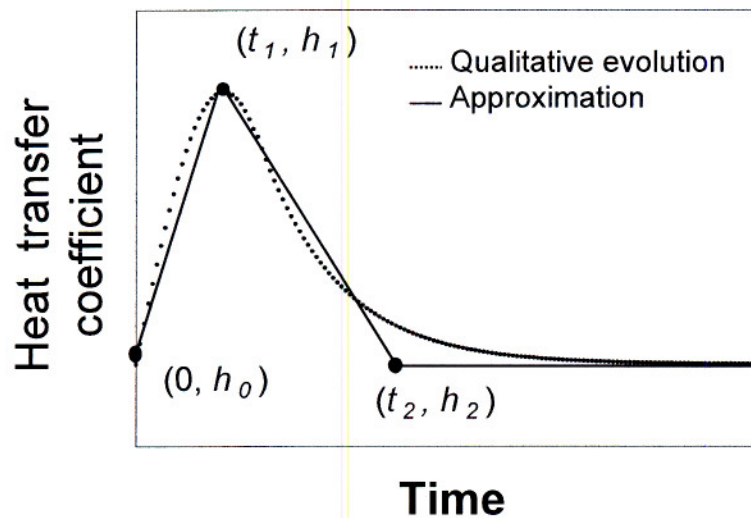

Figure 2 : Qualitative and approximated evolution of the heat transfer coefficient for a metal solidifying on a mold wall.

Experimental Procedure

As listed in Table 1 of the previous section, 16 different experimental conditions were investigated. Each experiment was performed twice for a total of 32 tests. The effect of two proprietary crucibles was evaluated along with two coatings applied at the interface between the crucible and the billet, two draining grids and two refractory bottom plates for the crucibles. The aluminum alloy that was utilized was the A356 and the crucibles had diameters and lengths fixed at 76 and 200 mm, respectively.

The experimental procedure was the same for the 32 tests. Ingots of the A356 alloy were first melted in a resistance furnace to a temperature of 700°C. Approximately 2.5 kg of liquid aluminum was ladled from the furnace with a spoon and a thermocouple was inserted into the molten aluminum it contained. When the desired temperature was reached, the SEED crucible was tilted to 45° and filled to the edge with aluminum. The crucible was then put in an upright position providing a metal height close to 150 mm. The crucible and the aluminum were swirled at 150 rpm during 45 s followed by a 10 s rest and a 45 s drainage. The last step was performed by sliding a gate at the bottom of the crucible. After drainage, the crucible was turned upside down so the billet could slide out.

Thermocouples in contact with the crucibles and inserted in the billets were used to provide the data for the inverse heat transfer calculations. Three type K surface thermocouples (Omega, model 88006) were installed against the external wall of the crucible and at different heights (75, 110 and 140 mm). Two type K grounded thermocouples were also located inside the semi-solid billet at mid-height. One was placed in the center of the billet and the other at 6 mm from the wall. The temperatures were recorded with a data acquisition system at a frequency of 10 Hz.

Results and Discussion

Figure 3 illustrates a typical evolution of the temperature given by the five thermocouples. Similar graphs were obtained for each experiment. The initial time, $t = 0$, was adjusted to correspond to the onset of the temperature rise detected by the thermocouples in the billet. Figure 4 depicts the heat flux evolution at the interface between the aluminum slug and the crucible. The curve was calculated on de basis of the temperature measurements presented in Figure 3 using the inverse method. The 2 regimes, transient and steady state, presented earlier in Figure 2 for the heat transfer coefficient can also be observed.
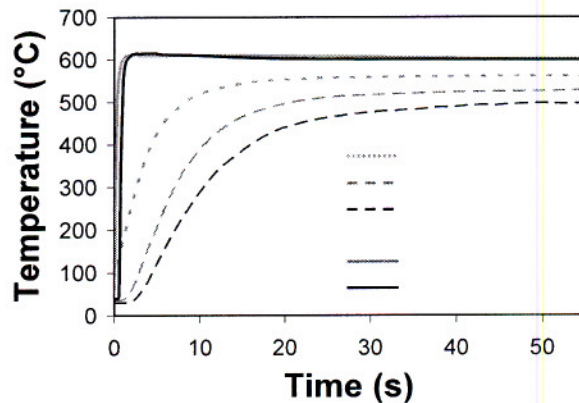
Figure 3 : Temperature evolution in the aluminum slug and at the surface of the crucible.
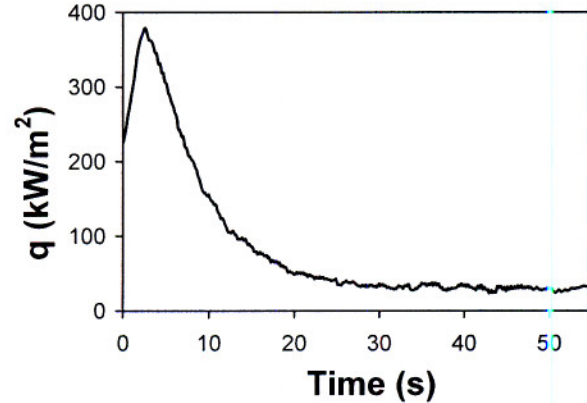
Figure 4 : Heat flux evolution at the crucible/billet interface.

Figure 5 illustrates the evolution of the heat transfer coefficient between the billet and the crucible with respect to time. As with the heat flux evolution, the transient and steady states are also present. The rapid fall in the coefficient is normally attributed to the formation of a gap between the solidifying material and its substrate [14]. This suggests that the slurry in the SEED crucible could have sufficient strength to contract away from the crucible wall. Also featured in Figure 5 is an idealized curve consisting of three linear segments; two of them representing the transient regime and the third, the steady one. The five response variables (h_0, t_1, h_1, t_2, h_2) are also identified and the effects of the experimental factors listed in Table 1 were evaluated for each of them.

Figure 6 is an example of a diagram constructed to evaluate the effects of the experimental factors on the response variable h_0. It consists in a Pareto chart obtained from the statistical analysis of the entire experimental data [15]. The classification is based of the F test with a significance level of 5% in the F-distribution ($\alpha = 0.05$). Factors in this figure having a standardized effect greater than 2.55 have a significant effect on the response variable h_0. It can be observed here that only the wall thickness of the crucible, H, is significant. Similar Pareto charts were also constructed for the other response variables t_1, h_1, t_2 and h_2.
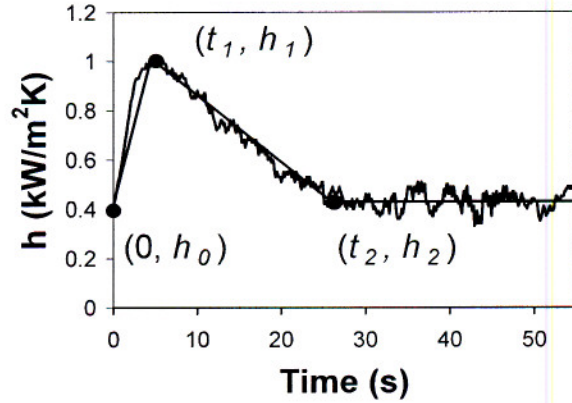
Figure 5 : Evolution of the heat transfer coefficient with respect to time with approximation using linear segments.
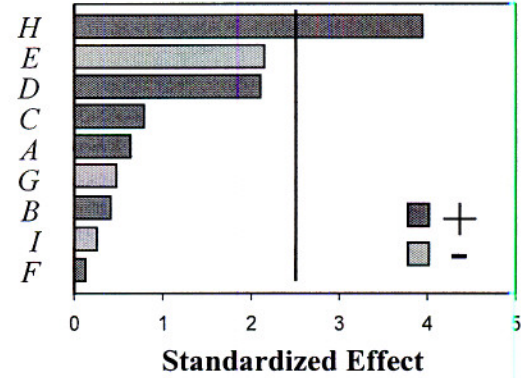

Figure 6 : Pareto diagram for h_0 illustrating the standardized effect. Letters on the ordinate refer to the experimental factors in Table 1.

Linear models were built for each response variable once their significant factors were identified and are shown in Table 2. It is noticed that only three experimental factors have an effect: the crucible wall thickness, H, the aluminum pouring temperature, B, and the proprietary coating, F. The latter is treated as a non-numeric label and can take the value of either 1 or 2, depending on the coating. The effects of the other process parameters are not significant in the range they were varied. It can also be observed that the steady state value of the heat transfer coefficient, h_2, remains constant (0.57 kW/m^{2}K) regardless of the experimental conditions. It is important to realize that this model is empirical, e.i., it only captures the trend of the data and is used to predict the coefficients and not to explain them. Other authors have used a different approach to build a model predicting heat transfer coefficients [16,17].

Response variables	Equations
h_0 (kW m^{-2} K^{-1})	$-0.01 + 0.22 \cdot H$
h_1 (kW m^{-2} K^{-1})	$0.86 + 0.19 \cdot H$
h_2 (kW m^{-2} K^{-1})	0.57
t_1 (s)	$22.41 - 0.02 \cdot B - 1.07 \cdot F$
t_2 (s)	$13.23 + 5.72 \cdot H$

Table 2 : Linear models for each response variable. Letters in equations refer to the experimental factors in Table 1.

A heat transfer coefficient curve can be constructed from the equations in Table 2 by inserting the values of the required process parameters. As discussed earlier, this coefficient is necessary to perform numerical simulations of temperature evolutions in the SEED process. Figure 7 depicts the calculated temperatures in a billet obtained with the ProCAST^{TM} finite element software along with the measured temperatures. The multiplying factor for the thermal conductivity of the liquid phase, k_c, was fixed to 5 in the model as the agreement between the simulations and the experiments did not justify using a higher value. Although the simulation results are well validated by the measurements, it should be realized that the value of the interfacial billet/crucible heat transfer coefficient was adjusted to reproduce the measured temperatures. The methodology used in this

work is thus one where the heat transfer model has adjustable parameters which are fitted to the experimental measurements. Figure 7 also shows a sensitivity analysis for the heat transfer coefficient where it was varied by ±15% to evaluate how it affected the temperature evolution. This change introduced a variation of ±2°C after 55 seconds of cooling.
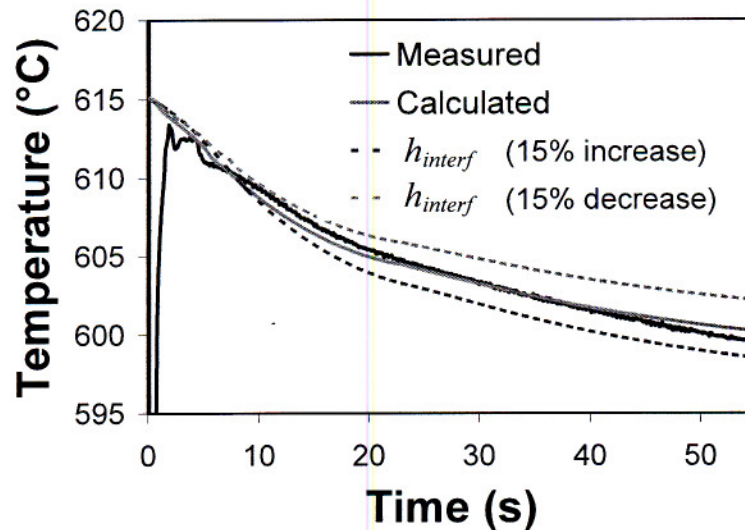

Figure 7 : Comparison of the measured and the calculated aluminum temperature in the billet and sensitivity analysis of the heat transfer coefficient on the temperature evolution.

It should be observed that the experimental measurements in Figure 7 are the average temperatures provided by the two thermocouples inserted in the billets. To perform the simulations, an initial temperature for the aluminum is required and the highest value given by either thermocouple from the experiments was used for that purpose. The simulations thus assumed that the crucible was initially full and the pouring temperature of the liquid aluminum given in Table 1 was not utilized since there is heat loss with an accompanying temperature drop during pouring. Work is presently carried out to predict the initial temperature of the aluminum after it is poured in a crucible. The present version of the model however provides a predictive tool to determine the temperature evolution in the billet for a given crucible mass and dimension. Each numerical simulation required one central processing unit (CPU) and approximately took two minutes on a Pentium 4 (3.00 GHz) computer. Time and efforts are then saved by performing numerical simulations to determine if a crucible provides the desired temperature evolution in the billet. Final experimental validations are required but the number of trials is reduced. Research is also carried out to determine the evolution of the solid fraction in the SEED billets. Presently, the solid fractions are determined from the temperatures assuming that the Scheil relationship [18] holds but this requires validation. A predictive model for drainage is also under evaluation and Darcy's law, typically applied to describe the flow of a liquid through a porous medium [19], is examined.

Conclusions

A heat transfer model for the production of semi-solid aluminum with the SEED process was built. Three factors were found to have a significant effect on the heat transfer coefficient at the interface between the SEED crucible and the aluminum billet: the crucible wall thickness, the initial pouring temperature, and the proprietary coatings. The simulations performed with the heat transfer model were well validated by the experimental measurements. Further work is presently carried out to model the evolution of the solid fractions and drainage.

Acknowledgments

References

[1] A. De Figueredo: *Science and technology of semi-solid metal processing* (North American Die Casting Association, USA 2001).

[2] D. Doutre, G. Hay and P. Wales, US Patent No. 6,428,636 (2002)

[3] J. Langlais, D. Doutre and S. Roy, Proceedings of the 8th International Conference on Semi-Solid Processing of Alloys and Composites, Limassol, Cyprus, September 21-23 (2004)

[4] J. Langlais, A. Lemieux, D. Bouchard and C. Sheehy, Proceedings of the SAE 2006 World Congress & Exhibition, Detroit, USA (2006) *to be published*

[5] D. Bouchard, F. Pineau, D. Doutre, P. Wales and J. Langlais, International Symposium on Light Metals, 42nd Annual Conference of Metallurgists of CIM, Vancouver, Canada, 24-27 Aug. (2003), pp. 229-241

[6] F. P. Incropera and D. P. DeWitt: *Fundamentals of Heat and Mass Transfer* (Wiley, USA 2002).

[7] B. Lally, L. Biegler and H. Henein, Metal. Trans. Vol. 21B (1990), pp. 761-770

[8] *Thermal Properties of Metals* (ASM International, USA 2002).

[9] D. R. Gaskell: *An Introduction to Transport Phenomena in Materials Engineering* (McMillan Publishing Company, USA 1992).

[10] J. V. Beck, B. Blackwell, C. R. St. Clair: *Inverse Heat Conduction* (Wiley-Interscience Publication, USA 1985).

[11] J.P. Holman: *Experimental Methods for Engineers* (McGraw-Hill, USA 2001).

[12] C. A. Muojekwu, I. V. Samarasekera and J. K. Brimacombe, Metallurgical and Materials Transaction B Vol. 26B no. 2 (1995), pp. 361-382

[13] J. S. Kim, M. Isac, R. I. L. Guthrie and J. Byun, Canadian Metallurgical Quarterly Vol. 41 no. 1 (2004), pp. 87-96

[14] P. Schmidt and I. L. Svensson, Numerical Methods in Thermal Problems, Vol. VII : Proceedings of the Seventh International Conference, Stanford, Connecticut, USA, 8-12 July (1991), pp. 236-247

[15] *Statgraphics Plus 5* (Mangistics Inc., USA 2000).

[16] W. D. Griffiths, Metallurgical and Materials Transaction B Vol. 31B (2000), pp. 285-295

[17] C. P. Hallam and W. G. Griffiths, Metallurgical and Materials Transaction B Vol. 35B (2004), pp. 721-733

[18] W. Kurz and D. J. Fischer: *Fundamentals of Solidification* (Trans Tech Publications, Switzerland 1986).

[19] R. W. Lewis, P. Nithiarasu and K. N. Seetharamu: *Fundamentals of the Finite Element Method for the Heat and Fluid Flow* (John Wiley & Sons Ltd, USA 2004).